HHS Public Access

Author manuscript

Mol Neurobiol. Author manuscript; available in PMC 2017 July 20.

Published in final edited form as:

Mol Neurobiol. 2015 October ; 52(2): 1023–1033. doi:10.1007/s12035-015-9252-9.

Exacerbation of Methamphetamine Neurotoxicity in Cold and Hot Environments: Neuroprotective Effects of an Antioxidant Compound H-290/51

Hari S Sharma[1,*], **Eugene A Kiyatkin**[2], **Ranjana Patnaik**[1,3], **Jose Vicente Lafuente**[4], **Dafin F Muresanu**[5], **Per-Ove Sjöquist**[6], and **Aruna Sharma**[1]

[1]Laboratory of Cerebrovascular Research, Dept. of Surgical Sciences, Anesthesiology & Intensive Care Medicine, University Hospital, Uppsala University, SE-75185 Uppsala, Sweden

[2]In-Vivo Electrophysiology Unit, Behavioral Neuroscience Branch. National Institute on Drug Abuse (NIDA)-Intramural Research Program (IRP), National Institute of Health, Baltimore, MD, USA

[3]Indian Institute of Technology, School of Biomedical Engineering, Dept. of Biomaterials, Banaras Hindu University, Varanasi-221005, India

[4]Dept Neurosciences, University of Basque Country, Bilbao, Spain

[5]Dept of Clinical Neurosciences, University Hospital, University of Medicine & Pharmacy, Cluj-Napoca, Romania

[6]Divison of Cardiology, Department of Medicine, Karolinska Institutet, Karolinska University Hospital, Stockholm, Sweden

Abstract

In this study, we examined the influence of cold and hot environments on methamphetamine (METH) neurotoxicity in both drug-naive rats and animals previously exposed to different types of nanoparticles (NPs). Since METH induces oxidative stress, we also examined how a potential chain-braking antioxidant H-290/51 (Astra-Zeneca Mölndal, Sweden) affects METH-induced neurotoxicity. Exposure of drug-naive rats to METH (9 mg/kg, s.c.) at 4°, 21° or 34°C for 3 hrs resulted in breakdown of the blood-brain barrier (BBB), brain edema and neuronal injuries, which all differed in their extent depending upon ambient temperatures. The changes were moderate at 21°C, 120–180% larger at 34°C, and almost absent at 4°C. In rats chronically treated with NPs (SiO2, Cu or Ag; 50–60 nm, 50 mg/kg, i.p. for 7 days), METH-induced brain alterations showed a 2- to 4-fold increase in brain pathologies after METH at 21°C; 4-to 6-fold increase at 34°C and 3- to 4-fold increase at 4°C. SiO2 exposure showed the most pronounced METH-induced brain pathology at all temperature ranges followed by Ag and Cu NPs. Pretreatment with a potent antioxidant compound H-290/51 (50 mg/kg, p.o. 30 min before METH) significantly reduced brain pathology in naive animals exposed to METH at 21°C and 34°C. In NPs-treated animals, however, attenuation of METH-induced brain pathology occurred only after repeated exposure of

[*]Correspondence: Hari Shanker Sharma, Ph D (BHU), Dr Med Sci (UU), Prof. of Neurobiology (MRC); Director of Research, Int. Exp. CNS Injury & Repair (IECNSIR), Uppsala University Hospital, Frödingsgatan 12, SE-75421 Uppsala, Sweden, Phone: +46 70 2011 801; Fax: +46 18 243899, Sharma@surgsci.uu.se.

H-290/51 (−30 min, 0 min and +30 min). These observations are the first to show that NPs aggravate METH-induced brain pathology in both cold and hot environments and demonstrate that timely intervention with antioxidant H-290/51 could have neuroprotective effects.

Keywords

methamphetamine; ambient temperature; nanoparticles; cold environment; hot environment; blood-brain barrier; brain edema; neuronal injury; antioxidants; H-290/51; oxidative stress

Introduction

Methamphetamine (METH) is increasingly abused by people living in both warm and cold environments and its use often results in not only behavioral or asocial activities, but also adverse health outcomes [1–8]. Often, METH is consumed by people exposed to a wide variety of nanoparticles (NPs) from either environmental or industrial sources, thus making them more vulnerable to METH-induced alterations in brain functions and behaviors [9–13]. Thus, it is critical to examine how the neural effects of METH are modulated in different temperature environments, how they are changed under conditions of NPs exposure, and how they could be pharmacologically corrected to attenuate harmful effects of METH on brain and behavior [10–16]. Previous experiments from our laboratory showed that engineered NPs from metals e.g., Ag or Cu enhanced brain trauma or METH neurotoxicity when given to rats at standard ambient temperatures [17–20]. However, it is unclear how NPs exposure could affect METH neurotoxicity or behavioral disturbances at hot and cold environmental temperatures.

Our previous work suggests that METH (9 mg/kg, s.c.) administered to rats at standard ambient temperatures (21–22°C) induces profound leakage of the blood-brain barrier (BBB), brain edema and cell injuries; these effects are strongly potentiated at warm ambient temperatures (29°C) [21–23]. While these data suggest that heat stress potentiates METH neurotoxicity, data on the influence of cold stress are lacking. Therefore, it is of great interest and practical importance to investigate the influence and interaction between environmental temperature, METH-induced neurotoxicity, and chronic NPs exposure. As both METH and NPs induce oxidative stress [24–27], an antioxidant may mitigate METH-induced neural changes and attenuate the potentiation of METH-induced neurotoxicity by chronic NPs exposure.

In the present study, we examined different neural parameters related to neurotoxicity after METH administration at low (4°C), standard (21°C) and high (34°) environmental temperatures in both normal animals and those previously chronically exposed to different types of NPs. We have chosen silica dust (SiO2), Silver (Ag) and Copper (Cu) NPs in the size range of 50–60 nm in order to see whether NP composition and particle size have specific effects on METH-induced neurotoxicity. In addition, we examined if and how a potent chain-breaking antioxidant compound (H-290/51, Astra-Zeneca, Mölndal, Sweden) might affect METH-induced neurotoxicity in both normal and NPs-exposed rats.

Materials and Methods

Animals

Experiments were carried out on male Sprague Dawley rats (220–260 g body weight) housed in a controlled ambient temperature (21±1°C) with 12 h light and 12 h dark schedule. Rats were supplied with food and water *ad libitum*. All experiments were conducted according National Institute of health (NIH) Guidelines and care of Experimental Animals and approved by Local Institutional Ethics Committee for animal experimentation [28].

Methamphetamine Administration

(+)-Methamphetamine hydrochloride (Sigma-Aldrich, M8750) was freshly dissolved in saline before use and administered subcutaneously (9 mg/kg, s.c.) at the dose 9 mg/kg. The rats were allowed to survive 3 h after the METH administration [21–23].

Exposure of rats at cold and hot ambient temperatures

Following METH or saline administration, separate groups of rats were placed in an environment-controlled chamber Comprehensive Lab Animal Monitoring System (CLAMS, Columbus Instruments, Columbus, OH, USA) at either 4°C or 34°C for 3 hrs. Other groups of rats after METH/Saline administration remained housed at a room temperature (21°C). There were no differences in BBB permeability or brain pathology between METH-experienced rats kept either at room temperature (21°C) or placed in environment-controlled chambers at 21°C (Sharma HS, unpublished observations). Thus, all the following experiments were conducted at room temperature (21°C).

Administration of Nanoparticles

Engineered nanoparticles (NPs) e.g., Copper (Cu), Silver (Ag) and silica dust (SiO2) were commercially procured from Denzlingen, Germany and cover a range between 50 to 60 nm. The size of nanoparticles was checked using transmission electron microscopy as described earlier [29, 30]. The nanoparticles were suspended in 0.05 % Tween 80 in 0.7% NaCl solution. In a separate group of rats, Ag, Cu or SiO2 NPs were administered 50 mg/kg, i.p. once daily for 1 week. On the 8th day these animals were subjected to METH administration (9 mg/kg, s.c.) at 4 °C, 21°C, and 34°C for 3 hrs.

Measured parameters

Blood-brain barrier permeability—The blood-brain barrier (BBB) breakdown was measured using Evans blue and radioiodine ([^{131}]$^{-}$Iodine) tracers that bind to serum proteins, largely albumin, when introduced into circulation [20–22]. Thus, leakage of these tracers across the BBB represents extravasation of serum-protein complexes. Evans blue dye (2 %, 0.3 ml/100 g) and radioiodine (106 CPM or 10 μCi/100g) were administered into the right femoral vein after the end of the experiment under Equithesin anesthesia (0. 3 ml/100 g, i.p.). After 5 to 8 min circulation of Evans blue and radioiodine tracers, the animals were perfused with 0.9% saline to washout the remaining blood from the blood vessels. Immediately before saline perfusion, about 1 ml of whole blood was withdrawn via cardiac

puncture for later determination of whole blood radioactivity [29]. After saline perfusion, the brain was dissected out and the extent of Evans blue dye spread in brain tissue was examined using a magnifying lens. The desired structures of the brain were then dissected out, weighed and radioactivity measured in a 3-in Gamma Counter (Packard, USA).

After measuring the radioactivity in the brain, samples were dissolved in a mixture of sodium sulphate and acetone to extract the Evans blue due that had entered into the brain. The samples were analyzed in spectrophotometer for colorimetric determination of Evans blue against the standard solution for the dye at 620 nm [20–22].

Brain edema formation—The brain edema formation was evaluated by measuring brain water content [20, 21]. Immediately after the brains were taken out, the desired areas of the brains were dissected out weighed and placed in an oven at 90°C for 72 h in order to evaporate the water content of the tissue. Dry weights of the samples were then recorded. The brain water content was calculated from the differences between the wet and dry weights of the samples. Volume swelling (% *f*) of the brain was calculated from the differences in brain water between the controls and experimental groups using the formula of Elliott & Jasper (1949) [31]. Approximately 1% increase in water corresponds to 4 % increase in volume swelling [see 21].

Morphological investigations

Neuronal injury—Neuronal injuries were examined using histopathological techniques on paraffin sections. After initial saline perfusion, animals were perfused with 4 % buffered paraformaldehyde (ca. 250 ml) at 90 Torr perfusion pressure using a peristaltic pump (Harvard Apparatus, USA). Animals were then wrapped in an aluminum foil and placed at 4°C in a refrigerator overnight. On the 2nd day, the brains were dissected out and placed in the same fixative at 4°C for one week. Then, 3- to 5-μm coronal sections passing through hippocampus were cut and embedded in paraffin using an automated tissue processor. About 3-μm thick paraffin sections were cut and stained with either Nissl or Haematoxylin & Eosin (H&E) for analyzing neuronal damages [20–22]. The images were examined in an Inverted Carl Zeiss Microscope and recoded on a digital camera (Olympus f 1.4). The images from control and experimental groups were analyzed using commercial Photoshop software (12.4.0) using identical filters [32].

Astrocytic reaction—Activation of astrocytes was examined by analyzing glial fibrillary acidic protein (GFAP) immunoreactivity using the standard commercial protocol [20–22]. In brief, 3-μm paraffin sections were deparaffinized and endogenous peroxidase was inhibited with 0.3 % hydrogen peroxide with 1 % non-immune horse serum in phosphate buffered saline (PBS, pH 7.4) for 20 min. Then, the sections were incubated for 8 h with monoclonal anti-GFAP serum (DAKO, Hamburg, Germany) diluted 1:500 in PBS at 4°C. After incubation with biotinylated horse anti-mouse immunoglobulin IgG at a 1:50 dilution and avidin-biotin complex (ABC) (Vector Laboratories, Burlingame, USA) for 45 min, the brown reaction product was developed with 3,3′-tetraaminobenzidine and hydrogen peroxide in 0.05 M Tris-HCl buffer (pH 7.4) for 4 min [33,34]. The paraffin sections of the control and METH-treated groups were processed in parallel. A few sections were

counterstained with Haematoxylin-Eosin for good contrast [34,35]. The GFAP immunoreactivity in selected areas of the brain was assessed in a blind fashion by two independent observers in a blinded fashion.

Treatment with H-290/51—The chain breaking antioxidant, H-290/51 (Astra-Zeneca, Mölndal, Sweden) was given to rats (50 mg/kg, p.o.) [36]. Various parameters were measured in order to evaluate the extent of METH-induced neurotoxicity as well as the influence of ambient temperature.

Physiological parameters

Skin and core body temperatures—The skin and core body temperatures were measured using thermistor probes (Yellow Springfield, USA) attached to a 12-channel telethermometer (Aplab Electronics, UK). Skin temperature (Ts) was recorded from tail and the core body temperature (Tc) was recorded by pacing the probe inside the rectum (approx. 4 cm). As such, deep visceral temperature was recorded both before and after the end of the experiments [37].

Cardiovascular parameters—The mean arterial blood pressure (MABP) was recorded at the end of the experiment from an indwelling cannula into the left carotid artery placed aseptically and retrogradely towards heart 7 days prior drug treatments. At the time of recording, the carotid artery catheter was connected to a Strain Gauge Pressure Transducer (Statham P23, USA) and connected to a chart recorder (Electromed, UK). At the time of MABP recording, both heart and respiration rates were also recorded using specific electrodes that were placed appropriately and connected with the chart recorder [37–39].

Arterial pH and blood gases—Immediately before MABP recording from the carotid artery catheter about 1 ml arterial blood was withdrawn for measurement of arterial pH and blood gases in a Radiometer Apparatus (Copenhagen, Denmark) [37].

Statistical analyses—ANOVA followed by Dunnett's test for multiple group comparison from one control was used to determine statistical significance of the data obtained. The statistical analyses were performed using Stat View 5 commercial software (Abacus concepts Inc. CA, USA) on a Macintosh Computer in a Classic Environment (System 9.8.6). A p-value less than 0.05 was considered significant.

Results

Methamphetamine induces blood-brain barrier breakdown and brain edema

METH administered to rats at standard room temperature (21°C) induced BBB disruption in several brain areas as it evident from Evans blue staining. Different areas of cerebral cortex, e.g., cingulate, frontal, occipital and temporal cortices, showed mild to moderate blue staining. The ventricular walls of the lateral ventricles were also stained. Mild blue staining was also seen in the hippocampus and caudate nucleus. Measurements of radioiodine extravasation and Evans blue leakage also showed significant increases compared to the drug-free control (Table 1). When METH was administered at hot ambient temperatures

(34°C), the intensity of the BBB breakdown was strongly increased, as evidenced by deeper Evans blue staining in these brain areas and significant increases in Evans blue levels. In this case, the piriform cortex, infundibulum, thalamus and hypothalamus also showed intense blue staining. Radioiodine extravasation was also enhanced significantly when METH was used at 34°C. However, METH administered at low ambient temperatures (4°C) induced only a very slight, not significant increase in Evans blue levels and $^{[131]-}$Iodine.

Although METH induced BBB leakage in all tested structures, the extent of radioiodine extravasation and its changes induced by METH was strongly influenced by different ambient temperatures (Table 2).

METH induced profound brain edema and volume swelling when exposed to METH at room temperature (Table 1). Both the brain water content and volume swelling significantly increased when the drug was used at 34° C. However, neither brain water content nor volume swelling was affected by <ETH under cold stress conditions (i.e. at 4°C).

Methamphetamine induces astrocytic activation and neuronal damage

METH treatment at 21°C resulted in the activation of astrocytes located in areas of neuronal damage (Table 1). Thus, the cerebral cortex, hippocampus and cerebellum showed several activated astrocytes that were GFAP-positive. Few GFAP-positive astrocytes were located in the perivascular areas in these brain regions. After METH at 34°C, the number of GFAP-positive astrocytes significantly increased and were found in several other brain areas, including the thalamus, hypothalamus, caudate nucleus and colliculi beside the cerebral cortex, hippocampus and cerebellum (Fig. 1a). Similar to other parameters, only a few astrocytes showed GFAP immunoreactivity in the cortex following METH injection at 4°C, and the difference vs. control was not significant.

METH administration at room temperature induced profound neuronal damages in several areas of the brain, including the cerebral cortex, hippocampus and cerebellum. These distorted neurons were largely located in the edematous areas of the brain which showed sponginess of the neuropil (Table 1 and Fig. 1a). These neuronal abnormalities were exacerbated in rats treated with METH 34°C. The damaged neurons in this group increased in number and the damage also extended to other brain areas, including the thalamus, hypothalamus, caudate nucleus and colliculi. Interestingly, rats treated with METH at 4°C showed only minimal neuronal injuries limited to cerebral cortex and the number of abnormal cells did not differ from 4°C control.

Nanoparticles exacerbate methamphetamine-induced brain pathology

Compared to the NPs-free controls, METH administered to NPs-exposed eats at room temperature induced much more robust changes in BBB permeability and glial activation, stronger brain edema, and more profound neuronal injuries (Table 1). Similar to intact rats, the changes in all parameters were lower when METH was administered at 4°C and higher at 34°C (see Fig. 1b). In contrast to intact animals, however, NPs-treated rats showed profound neuronal damage, BBB breakdown and edema formation after METH treatment in cold environment; the difference vs. 4°C control was significant for each parameter in each of the three NP groups. Interestingly, the rats exposed to SiO2 NPs exhibited higher brain

damage and stronger glial activation after METH administration at all ambient temperatures. The severity of brain damage and strength of glial activation was followed by Ag NPs and lastly Cu NPs. NPs exacerbated METH-induced neural responses in all tested structures, but the changes showed certain structural variability (Table 2).

Antioxidant compound H-290/51 induces neuroprotection

Pretreatment of rats with the chain-breaking antioxidant H-290/51 (50 mg/kg) 30 min before METH administration significantly reduced BBB breakdown, brain edema formation, and brain cell pathology in rats exposed to METH at either 21° or 34°C (Table 3). NPs-exposed rats, however, must be treated with H-290/51 three times-once 30 min before, immediately after, and 30 min following METH administration, in order to observe a reliable neuroprotective effect (see also Fig. 1c).

Physiological variables in METH-treated groups

METH treatment at room temperature induced profound hyperthermia as seen by increases in rectal (Tc) and skin (Ts) temperatures measured at 3 h (Table 4). The increases in Tc or Ts were enhanced when rats were placed at 34°C after METH administration. However, rats treated with METH at 4°C showed significant hypothermia; both Tc and Ts were greatly lowered versus the control group. However, in NPs-exposed rats METH-induced temperature increases were larger when the drug was administered at room and hot ambient temperatures. The decline in Tc and Ts seen at 4°C was considerably reduced.

Rats treated with METH at room temperature showed a slight increase in MABP and PaO2, whereas PaCO2 showed a mild decrease despite the fact that arterial pH remained unchanged. In a hot environment, METH resulted in a slightly larger rise in MABP (non significant change), whereas arterial pH and blood gases did not differ significantly from METH-treated rats at room temperature. On the other hand, METH administration in cold temperature resulted in a slight hypotension, but again the arterial pH and blood gases were not much affected. The heart and respiration rates were increased by METH use at room temperature. These increases were larger in a hot environment but much smaller in a cold environment.

Interestingly, NPs-exposed rats showed higher MABP, heart rate and respiration cycle at all temperature ranges (Table 4). However, the arterial pH did not change in NPs-exposed rats that received METH regardless of temperature. A slight increase in PaO2 and a significant decrease in PaCO2 were observed in METH-treated group after NPs intoxication, but this change was not affected further by either cold or hot exposure.

H-290/51 treatment did not significantly alter these physiological variables either in normal or NPs-exposed rats that received METH at any ambient temperatures (Table 4).

Discussion

METH is a drug of abuse with neurotoxic properties. Previous reports from our laboratory showed that METH resulted in the breakdown of the BBB and brain injury in both rats and mice [21–23, 40–42]. Our studies also showed that METH administered at warm ambient

temperatures (29°C) induced larger temperature increases and more severe neuronal injury [21–23, 43].

The present study confirms our previous work indicating that METH-induced neurotoxicity is temperature-dependent and further elucidates how temperature exposure drastically influences METH-induced neuronal responses. As such, METH administered at 34°C showed massive brain pathology as compared to METH administered at 21°C, but identical METH exposure at 4°C did not induced evident BBB breakdown and brain damage.

The primary novel finding of this study is that rats chronically exposed to NPs show much stronger METH-induced neural responses than intact animals at each of the ambient temperatures. Interestingly, in NPs-exposed rats, METH induced profound neurotoxicity at a low temperature—a feature absent in intact rats. Thus, NPs aggravate METH-induced neurotoxicity within the wide range of environmental temperatures.

The mechanisms by which NPs could exacerbate METH toxicity in both cold and hot environments are not well known. However, there are reasons to believe that hypothermia induced by METH at cold ambient temperatures is not neuroprotective. This is apparent from our finding that pentobarbital-anesthetized rats that have low brain and body temperatures showed considerable leakage of BBB to albumin and neuronal injuries [44]. Forced swim experiments, in which rats were allowed to swim at 30°C for 30 min, provide further evidence of BBB leakage despite lowered body temperature (~5°C decrease) [45,46]. Moreover, drugs that blocked the BBB leakage in this model did not prevent hypothermia induced by the forced swim test [45,46]. As such, hypothermia *per se* does not protect the brain from BBB damage caused by either forced swim or METH administration. The reduction or minimal damage done by METH at 4°C in rats may be due to an attenuation of drug-induced cellular and/or oxidative stress.

The dual role of temperature is further supported by our findings in NPs-exposed rats that received METH at 4°C. These rats did not show hyperthermia as their body temperature remained slightly below than the average in the control group. However, they exhibited massive BBB breakdown and brain pathology. Since NPs induce profound oxidative and cellular stress, it appears that a combination of METH and NPs could induce BBB breakdown even in a cold environment. Since NPs alone at 4°C did not induce BBB breakdown or neuronal injury, it seems likely that a combination of METH and NPs are needed to induce brain pathology in a cold environment.

This observation indicates that METH users that live in polluted environments may develop stronger mental anomalies or brain dysfunctions than METH users living in cleaner environment. Obviously, people that are exposed to silica dust and other NPs from industrial sources or gunpowder explosions could be more vulnerable to substance abuse and drug-induced deterioration of brain functions. However, further studies are needed in this area to prove these points.

As compared to Ag or Cu NPs exposure, we observed that SiO2 NPs exposure resulted in more profound BBB breakdown, stronger brain edema formation and larger neuronal or glial injuries following METH administration regardless of ambient temperature. This suggests

that the inherent properties of NPs might play a key role in brain dysfunctions induced by METH, although the exact mechanisms of such an interaction are unknown [47–49]. However, available evidences suggests that the zeta potential, electric charges and dispersion of NPs in biological or surrounding medium could determine the actual effects of NPs in any environment [50]. Previous studies also suggest that SiO2 NPs induce more robust neuronal reactions and more severe disruptions in BBB permeability during heat exposure and spinal cord injury than either Ag or Cu NPs [18,51,52]. The present results further support the idea that SiO2 NPs could also enhance METH-induced neurotoxicity as compared to other metal NPs i.e., Ag and Cu NPs.

The most likely cause for NPs-induced exacerbation of neurotoxic effects of METH is an enhanced oxidative stress in the CNS. This idea is supported by the fact that exposure to Cu, Ag or Al NPs during 4-hr whole body hyperthermia results in 4 to 6-fold increases in oxidative stress compared to saline-treated heat-exposed animals [53, Sharma HS unpublished observations]. Thus, it would be interesting to measure oxidative stress in animals exposed to METH with or without NPs at different ambient temperatures.

The role of oxidative stress in METH-induced neurotoxicity together with NPs intoxications is further supported by our observations with a potent antioxidant compound H-290/51. The H-290/51 is a chain-breaking antioxidant that is capable of attenuating spinal cord injury, neuronal damages, and edema formation in SiO2-treated rats [20, 51]. Based on these observations, we pretreated animals with H-290/51 and then administered METH at 21° and 34°C. Since H-290/51 was able to attenuate METH neurotoxicity in these animals, we believe that oxidative stress plays an important role in METH-induced neurotoxicity. However, when METH was used in NPs-exposed rats, repeated treatment with H290/51 or higher doses of the drug was necessary to reduce METH neurotoxicity at cold, neutral or hot ambient temperatures. This confirms the idea that NPs intoxication induces additional oxidative stress that requires a higher dose of the antioxidant to induce neuroprotection.

NPs could be used as an effective tool to deliver therapeutic drugs in brain tissue. We have shown earlier that TiO2-nanowired delivery of drugs during CNS trauma has a superior neuroprotective effect than the traditional drug delivery [54–58]. It could be of interest to examine whether nanowire drug delivery of H290/51 could be more effective in attenuating METH-induced neurotoxicity at different ambient temperatures. This work is currently in progress in our laboratory.

In conclusion, our results are the first to show that NPs intoxication exacerbates METH-induced neurotoxicity that occurs in both cold and hot environments. This METH-induced neurotoxicity could be possibly prevented by the timely administration of antioxidant compound H-290/51. This indicates that oxidative stress plays an important role in METH-induced neurotoxicity and is exacerbated by NPs intoxication, a finding not reported earlier.

Acknowledgments

This investigation is supported by grants from the Air Force Office of Scientific Research (EOARD, London, UK), and Air Force Material Command, USAF, under grant number FA8655-05-1-3065; Swedish Medical Research Council (Nr 2710-HSS), Swedish Strategic Research Foundation, Stockholm, Sweden; Göran Gustafsson Foundation, Stockholm, Sweden (HSS), Astra Zeneca, Mölndal, Sweden (HSS/AS), The University Grants

Commission, New Delhi, India (HSS/AS), Ministry of Science & Technology, Govt. of India & Govt. of Sweden (HSS/AS), Indian Medical Research Council, New Delhi, India (HSS/AS); India-EU Research Co-operation Program (RP/AS/HSS) and IT 794/13 (JVL), Government of Basque Country and UFI 11/32 (JVL); University of Basque Country, Spain.

References

1. Ellinwood EH, Cohen S. Amphetamine abuse. Science. 1971; 171(3969):420–1. [PubMed: 4923360]
2. Marquine MJ, Iudicello JE, Morgan EE, Brown GG, Letendre SL, Ellis RJ, Deutsch R, Woods SP, Grant I, Heaton RK. Translational Methamphetamine AIDS Research Center (TMARC) Group. "Frontal systems" behaviors in comorbid human immunodeficiency virus infection and methamphetamine dependency. Psychiatry Res. 2014 Jan 30; 215(1):208–16. [PubMed: 24290100]
3. Lecomte T, Mueser KT, MacEwan W, Thornton AE, Buchanan T, Bouchard V, Goldner E, Brink J, Lang D, Kang S, Barr AM, Honer WG. Predictors of persistent psychotic symptoms in persons with methamphetamine abuse receiving psychiatric treatment. J Nerv Ment Dis. 2013 Dec; 201(12): 1085–9. DOI: 10.1097/NMD.0000000000000059 [PubMed: 24284645]
4. Fletcher JB, Reback CJ. Antisocial personality disorder predicts methamphetamine treatment outcomes in homeless, substance-dependent men who have sex with men. J Subst Abuse Treat. 2013 Sep; 45(3):266–72. Epub 2013 Apr 8. DOI: 10.1016/j.jsat.2013.03.002 [PubMed: 23579078]
5. Embry D, Hankins M, Biglan A, Boles S. Behavioral and social correlates of methamphetamine use in a population-based sample of early and later adolescents. Addict Behav. 2009 Apr; 34(4):343–51. Epub 2008 Nov 27. DOI: 10.1016/j.addbeh.2008.11.019 [PubMed: 19138821]
6. Iritani BJ, Hallfors DD, Bauer DJ. Crystal methamphetamine use among young adults in the USA. Addiction. 2007 Jul; 102(7):1102–13. [PubMed: 17567398]
7. Jones HE, Myers B, O'Grady KE, Gebhardt S, Theron GB, Wechsberg WM. Initial feasibility and acceptability of a comprehensive intervention for methamphetamine-using pregnant women in South Africa. Psychiatry J. 2014; 2014:929767. Epub 2014 Jan 5. doi: 10.1155/2014/929767 [PubMed: 24829904]
8. Werb D, Kerr T, Buxton J, Shoveller J, Richardson C, Montaner J, Wood E. Crystal methamphetamine and initiation of injection drug use among street-involved youth in a Canadian setting. CMAJ. 2013 Dec 10; 185(18):1569–75. Epub 2013 Oct 15. DOI: 10.1503/cmaj.130295 [PubMed: 24130244]
9. Shariatirad S, Maarefvand M, Ekhtiari H. Emergence of a methamphetamine crisis in Iran. Drug Alcohol Rev. 2013 Mar; 32(2):223–4. Epub 2012 Nov 28. DOI: 10.1111/dar.12014 [PubMed: 23190186]
10. Li L, Assanangkornchai S, Duo L, McNeil E, Li J. Cross-border activities and association with current methamphetamine use among Chinese injection drug users (IDUs) in a China-Myanmar border region. Drug Alcohol Depend. 2014 May 1.138:48–53. Epub 2014 Feb 12. DOI: 10.1016/j.drugalcdep.2014.01.021 [PubMed: 24629780]
11. Shukla RK, Crump JL, Chrisco ES. An evolving problem: methamphetamine production and trafficking in the United States. Int J Drug Policy. 2012 Nov; 23(6):426–35. Epub 2012 Sep 1. Review. DOI: 10.1016/j.drugpo.2012.07.004 [PubMed: 22943831]
12. Verdichevski M, Burns R, Cunningham JK, Tavares J, Callaghan RC. Trends in primary methamphetamine-related admissions to youth residential substance abuse treatment facilities in Canada, 2005–2006 and 2009–2010. Can J Psychiatry. 2011 Nov; 56(11):696–700. [PubMed: 22114924]
13. Forcehimes AA, Venner KL, Bogenschutz MP, Foley K, Davis MP, Houck JM, Willie EL, Begaye P. American Indian methamphetamine and other drug use in the Southwestern United States. Cultur Divers Ethnic Minor Psychol. 2011 Oct; 17(4):366–76. DOI: 10.1037/a0025431 [PubMed: 21988577]
14. Platteborze PL, Kippenberger DJ, Martin TM. Drug positive rates for the Army, Army Reserve, and Army National Guard from fiscal year 2001 through 2011. Mil Med. 2013 Oct; 178(10):1078–84. DOI: 10.7205/MILMED-D-13-00193 [PubMed: 24083921]

15. Lacy BW, Ditzler TF, Wilson RS, Martin TM, Ochikubo JT, Roussel RR, Pizarro-Matos JM, Vazquez R. Regional methamphetamine use among U.S. Army personnel stationed in the continental United States and Hawaii: a six-year retrospective study (2000–2005). Mil Med. 2008 Apr; 173(4):353–8. [PubMed: 18472624]

16. Defalque RJ, Wright AJ. Methamphetamine for Hitler's Germany: 1937 to 1945. Bull Anesth Hist. 2011 Apr; 29(2):21–4. 32. [PubMed: 22849208]

17. Patnaik, R., Sharma, A., Kiyatkin, EA., Nozari, A., Sharma, HS. Nanoparticles exacerbate methamphetamine neurotoxicity in both hot or cold environment. Neuroprotective effects of an antioxidant compound H-290/51; 43rd Annual Meeting of the Society-for-Neuroscience; San Diego, CA, USA. November 09–13, 2013;

18. Sharma HS, Muresanu DF, Patnaik R, Sharma A. Exacerbation of brain pathology after partial restraint in hypertensive rats following SiO_2 nanoparticles exposure at high ambient temperature. Mol Neurobiol. 2013 Oct; 48(2):368–79. Epub 2013 Jul 6. DOI: 10.1007/s12035-013-8502-y [PubMed: 23832531]

19. Sharma HS, Muresanu DF, Sharma A, Patnaik R, Lafuente JV. Chapter 9 - Nanoparticles influence pathophysiology of spinal cord injury and repair. Prog Brain Res. 2009; 180:154–80. Epub 2009 Dec 8. Review. [PubMed: 20302834]

20. Sharma HS, Ali SF, Tian ZR, Hussain SM, Schlager JJ, Sjöquist PO, Sharma A, Muresanu DF. Chronic treatment with nanoparticles exacerbate hyperthermia induced blood-brain barrier breakdown, cognitive dysfunction and brain pathology in the rat. Neuroprotective effects of nanowired-antioxidant compound H-290/51. J Nanosci Nanotechnol. 2009 Aug; 9(8):5073–90. [PubMed: 19928186]

21. Kiyatkin EA, Brown PL, Sharma HS. Brain edema and breakdown of the blood-brain barrier during methamphetamine intoxication: critical role of brain hyperthermia. Eur J Neurosci. 2007 Sep; 26(5):1242–53. [PubMed: 17767502]

22. Sharma HS, Kiyatkin EA. Rapid morphological brain abnormalities during acute methamphetamine intoxication in the rat: an experimental study using light and electron microscopy. J Chem Neuroanat. 2009 Jan; 37(1):18–32. Epub 2008 Aug 19. [PubMed: 18773954]

23. Kiyatkin EA, Sharma HS. Acute methamphetamine intoxication: brain hyperthermia, blood-brain barrier, brain edema, and morphological cell abnormalities. Int Rev Neurobiol. 2009; 88:65–100. Review. [PubMed: 19897075]

24. Toborek M, Seelbach MJ, Rashid CS, András IE, Chen L, Park M, Esser KA. Voluntary exercise protects against methamphetamine-induced oxidative stress in brain microvasculature and disruption of the blood-brain barrier. Mol Neurodegener. 2013 Jun 24.8:22.doi: 10.1186/1750-1326-8-22 [PubMed: 23799892]

25. Solhi H, Malekirad A, Kazemifar AM, Sharifi F. Oxidative stress and lipid peroxidation in prolonged users of methamphetamine. Drug Metab Lett. 2014 Jul; 7(2):79–82. [PubMed: 24856264]

26. Patlolla AK, Hackett D, Tchounwou PB. Silver nanoparticle-induced oxidative stress-dependent toxicity in Sprague-Dawley rats. Mol Cell Biochem. 2014 Oct 30. Epub ahead of print.

27. Han JW, Gurunathan S, Jeong JK, Choi YJ, Kwon DN, Park JK, Kim JH. Oxidative stress mediated cytotoxicity of biologically synthesized silver nanoparticles in human lung epithelial adenocarcinoma cell line. Nanoscale Res Lett. 2014 Sep 2.9(1):459. eCollection 2014. doi: 10.1186/1556-276X-9-459 [PubMed: 25242904]

28. Committee for the Update of the Guide for the Care and Use of Laboratory Animals. 8. The National Academic Press; Washington DC: 2011. http://www.nap.edu

29. Sharma HS, Ali SF, Hussain SM, Schlager JJ, Sharma A. Influence of engineered nanoparticles from metals on the blood-brain barrier permeability, cerebral blood flow, brain edema and neurotoxicity. An experimental study in the rat and mice using biochemical and morphological approaches. J Nanosci Nanotechnol. 2009 Aug; 9(8):5055–72. [PubMed: 19928185]

30. Sharma HS, Sharma A. Nanoparticles aggravate heat stress induced cognitive deficits, blood-brain barrier disruption, edema formation and brain pathology. Prog Brain Res. 2007; 162:245–73. Review. [PubMed: 17645923]

31. Elliott KA, Jasper HH. Measurement of experimentally induced brain swelling and shrinkage. Am J Physiol. 1949 Apr; 157(1):122–9. [PubMed: 18130228]
32. Sharma HS, Sjöquist P-O. A new antioxidant compound H-290/51 modulates glutamate and GABA immunoreactivity in the rat spinal cord following trauma. Amino Acids. 2002; 23:261–272. [PubMed: 12373546]
33. Sharma HS, Olsson Y, Cervós-Navarro J. p-Chlorophenylalanine, a serotonin synthesis inhibitor, reduces the response of glial fibrillary acidic protein induced by trauma to the spinal cord. Acta Neuropathologica (Berlin). 1993; 86:422–427. [PubMed: 8310791]
34. Sharma HS, Zimmer C, Westman J, Cervós-Navarro J. Acute systemic heat stress increases glial fibrillary acidic protein immunoreactivity in brain. An experimental study in the conscious normotensive young rats. Neuroscience. 1992; 48:889–901. [PubMed: 1630627]
35. Zimmer C, Sampaolo S, Sharma HS, Cervós-Navarro J. Glial fibrillary acidic protein immunoreactivity in rat brain following chronic hypoxia. Neuroscience. 1991; 40:353–361. [PubMed: 2027465]
36. Mustafa A, Sharma HS, Olsson Y, Gordh T, Thoren P, Sjoquist PO, Roos P, Adem A, Nyberg F. Vascular permeability to growth hormone in the rat central nervous system after focal spinal cord injury. Influence of a new anti-oxidant H 290/51 and age. Neurosci Res. 1995 Sep; 23(2):185–94. [PubMed: 8532215]
37. Sharma HS, Dey PK. Influence of long-term acute heat exposure on regional blood-brain barrier permeability, cerebral blood flow and 5-HT level in conscious normotensive young rats. Brain Research. 1987; 424:153–162. [PubMed: 3690295]
38. Sharma HS, Dey PK. Influence of long-term immobilization stress on regional blood-brain barrier permeability, cerebral blood flow and 5-HT level in conscious normotensive young rats. Journal of the Neurological Sciences. 1986; 72:61–76. [PubMed: 2936871]
39. Sharma HS, Dey PK. Probable involvement of 5-hydroxytryptamine in increased permeability of blood-brain barrier under heat stress. Neuropharmacology. 1986; 25:161–167. [PubMed: 2939361]
40. Sharma HS, Ali SF. Alterations in blood-brain barrier function by morphine and methamphetamine. Ann N Y Acad Sci. 2006 Aug.1074:198–224. [PubMed: 17105918]
41. Sharma HS, Sjöquist PO, Ali SF. Drugs of abuse-induced hyperthermia, blood-brain barrier dysfunction and neurotoxicity: neuroprotective effects of a new antioxidant compound H-290/51. Curr Pharm Des. 2007; 13(18):1903–23. Review. [PubMed: 17584116]
42. Sharma HS, Menon P, Lafuente JV, Muresanu DF, Tian ZR, Patnaik R, Sharma A. Development of in vivo drug-induced neurotoxicity models. Expert Opin Drug Metab Toxicol. 2014 Oct.13:1–25. Epub ahead of print.
43. Kiyatkin EA, Sharma HS. Environmental conditions modulate neurotoxic effects of psychomotor stimulant drugs of abuse. Int Rev Neurobiol. 2012; 102:147–71. [PubMed: 22748829]
44. Kiyatkin EA, Sharma HS. Permeability of the blood-brain barrier depends on brain temperature. Neuroscience. 2009 Jul 7; 161(3):926–39. [PubMed: 19362131]
45. Sharma HS, Cervós-Navarro J, Dey PK. Increased blood-brain barrier permeability following acute short-term forced-swimming exercise in conscious normotensive young rats. Neuroscience Research. 1991; 10:211–221. [PubMed: 1650437]
46. Sharma HS, Westman J, Cervós-Navarro J, Dey PK, Nyberg F. Probable involvement of serotonin in the increased permeability of the blood-brain barrier by forced swimming. An experimental study using Evans blue and 131I-sodium tracers in the rat. Behavioural Brain Research. 1995; 72:189–196. [PubMed: 8788871]
47. Sharma A, Muresanu DF, Patnaik R, Sharma HS. Size- and age-dependent neurotoxicity of engineered metal nanoparticles in rats. Mol Neurobiol. 2013 Oct; 48(2):386–96. Epub 2013 Jul 3. DOI: 10.1007/s12035-013-8500-0 [PubMed: 23821031]
48. Sharma HS, Sharma A. Nanowired drug delivery for neuroprotection in central nervous system injuries: modulation by environmental temperature, intoxication of nanoparticles, and comorbidity factors. Wiley Interdiscip Rev Nanomed Nanobiotechnol. 2012 Mar-Apr;4(2):184–203. [PubMed: 22162425]
49. Sharma HS, Sharma A. New perspectives of nanoneuroprotection, nanoneuropharmacology and nanoneurotoxicity: modulatory role of amino acid neurotransmitters, stress, trauma, and co-

morbidity factors in nanomedicine. Amino Acids. 2013 Nov; 45(5):1055–71. DOI: 10.1007/s00726-013-1584-z [PubMed: 24022705]

50. Wang XZ, Yang Y, Li R, McGuinnes C, Adamson J, Megson IL, Donaldson K. Principal component and causal analysis of structural and acute in vitro toxicity data for nanoparticles. Nanotoxicology. 2014 Aug; 8(5):465–76. DOI: 10.3109/17435390.2013.796534 [PubMed: 23586395]
51. Sharma HS, Patnaik R, Sharma A, Sjöquist PO, Lafuente JV. Silicon dioxide nanoparticles (SiO2, 40–50 nm) exacerbate pathophysiology of traumatic spinal cord injury and deteriorate functional outcome in the rat. An experimental study using pharmacological and morphological approaches. J Nanosci Nanotechnol. 2009 Aug; 9(8):4970–80. [PubMed: 19928175]
52. Sharma HS, Sharma A. Neurotoxicity of engineered nanoparticles from metals. CNS Neurol Disord Drug Targets. 2012 Feb; 11(1):65–80. Review. [PubMed: 22229317]
53. Sharma A, Muresanu DF, Mössler H, Sharma HS. Superior neuroprotective effects of cerebrolysin in nanoparticle-induced exacerbation of hyperthermia-induced brain pathology. CNS Neurol Disord Drug Targets. 2012 Feb; 11(1):7–25. Review. [PubMed: 22229316]
54. Sharma HS. Early microvascular reactions and blood-spinal cord barrier disruption are instrumental in pathophysiology of spinal cord injury and repair: novel therapeutic strategies including nanowired drug delivery to enhance neuroprotection. J Neural Transm. 2011 Jan; 118(1):155–76. Epub 2010 Dec 16. Review. [PubMed: 21161717]
55. Tian ZR, Sharma A, Nozari A, Subramaniam R, Lundstedt T, Sharma HS. Nanowired drug delivery to enhance neuroprotection in spinal cord injury. CNS Neurol Disord Drug Targets. 2012 Feb; 11(1):86–95. Review. [PubMed: 22385571]
56. Muresanu DF, Sharma A, Tian ZR, Smith MA, Sharma HS. Nanowired drug delivery of antioxidant compound H-290/51 enhances neuroprotection in hyperthermia-induced neurotoxicity. CNS Neurol Disord Drug Targets. 2012 Feb; 11(1):50–64. Review. [PubMed: 22229325]
57. Sharma, A., Muresanu, DF., Lafuente, JV., Menon, P., Patnaik, R., Tian, ZR., Mössler, H., Sharma, HS. Nanodelivery of cerebrolysin as adjunct therapy with functionalized magnetic iron oxide nanoparticles enhances neuroprotection following whole body hyperthermia. In Proceedings National Innovations Summit & Showcase; National Harbor, Washington DC. June 15–18, 2014; 2014. p. 363-366.Technical Innovation Nr. 613. Advanced Materials & Applications, NSTI-Nanotech 2014www.nsti.org
58. Ruozi B, Belletti D, Forni F, Sharma A, Muresanu D, Mössler H, Vandelli MA, Tosi G, Sharma HS. Poly (D,L-lactide-co-glycolide) Nanoparticles Loaded with Cerebrolysin Display Neuroprotective Activity in a Rat Model of Concussive Head Injury. CNS Neurol Disord Drug Targets. 2014 Aug 6.

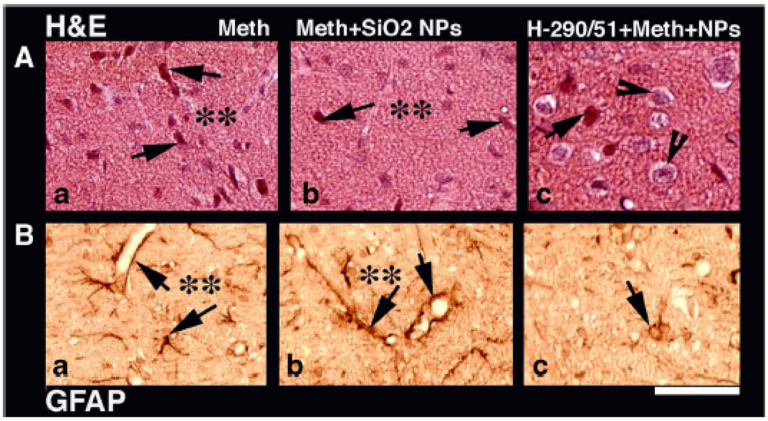

Figure 1.

Neuronal damage (H&E staining, upper panel) and glial activation (GFAP immunoreactivity; lower panel) induced by methamphetamine administered at 34° C (a). SiO2 NPs exposure exacerbates METH-induced neuronal loss and enhances GFAP activation in the neuropil and around the micro vessels (b). Repeated treatment with H-290/51 markedly reduces neuronal loss as many healthy nerve cells are seen in the neuropil (c). Moreover, this treatment decreases activation of GFAP around microvessels, with only a few nerve cells are stained with GFAP (c). Bar = 34 μm.

Mol Neurobiol. Author manuscript; available in PMC 2017 July 20.

Table 1

METH neurotoxicity is dependent on ambient temperature and enhanced after nanoparticle administration

Groups	BBB breakdown		Brain Edema		Brain Pathology	
	Evans Blue, mg%	[131]-Iodine, %	Water content, %	% *f*	Neuronal Damage Abnormal cells	Astrocytic activation GFAP-positive cells
Control						
Saline 4°C	0.18±0.06	0.28±0.07	75.03±0.10	nil	2±1	3±2
Saline 21°C	0.20±0.04	0.30±0.04	75.11±0.12	nil	2±3	3±4
Saline 34°C	0.22±0.06	0.32±0.06	75.24±0.17	nil	3±4	4±3
METH						
METH 4°C	0.24±0.08***	0.45±0.08***	75.04±0.12**	nil	4±2***	6±8**
METH 21°C	1.89±0.21^{o}	2.34±0.23^{ooo}	76.34±0.21^{oo}	+4	80±12^{ooo}	65±14^{ooo}
METH 34°C	2.67±0.26*,^{ooo}	3.45±0.23**,^{ooo}	77.45±0.12**,^{ooo}	+8	140±13***,^{ooo}	120±18*,^{ooo}
Nanoparticles+METH						
SiO2 NPs						
METH 4°C	1.78±0.21^{ooo}	2.46±0.21^{ooo}	78.23±0.45*,^{ooo}	+12	220±34*,^{ooo}	190±32**,^{ooo}
METH 21°C	2.45±0.33	2.98±0.10	79.56±0.21^{ooo}	+17	367±43^{ooo}	345±28^{ooo}
METH 34°C	3.21±0.21	3.87±0.11***	80.54±0.22***,^{ooo}	+23	456±28^{ooo}	398±12^{ooo}
Ag NPs						
METH 4°C	1.34±0.10***,^{ooo}	2.34±0.22^{ooo}	77.56±0.21***,^{ooo}	+8	160±33**,^{ooo}	187±27*,^{ooo}
METH 21°C	2.24±0.08	2.78±0.12	78.87±0.18^{ooo}	+13	308±26^{ooo}	298±32^{ooo}
METH 34°C	3.01±0.09***	3.45±0.09***	79.85±0.21**,^{ooo}	+16	412±34*,^{ooo}	325±28^{ooo}
Cu NPs						
METH 4°C	1.23±0.07***,^{ooo}	2.12±0.10***,^{ooo}	77.34±0.12**,^{ooo}	+8	140±23***,^{ooo}	167±24*,^{ooo}
METH 21°C	2.06±0.06	2.65±0.07	78.08±0.16^{ooo}	+12	280±18^{ooo}	245±26^{ooo}
METH 34°C	2.89±0.10	3.12±0.09***	79.21±0.12***,^{ooo}	+21	378±23***,^{ooo}	312±20*,^{ooo}
Saline+Nanoparticles						
Saline 21°C						
SiO2 NPs	0.23±0.08	0.34±0.07	75.28±0.21	nil	4±3	6±4
Ag NPs	0.26±0.07	0.36±0.10	75.32±0.24	nil	5±3	6±3
Cu NPs	0.24±0.04	0.35±0.08	75.24±0.18	nil	6±4	7±3

Values are mean±SEM obtained from 5 to 8 rats at each point. Volume swelling (% Δ) was calculated according to Elliott & Jasper [31] and adjusted to nearest round figure for simplicity. Asterisks show significant differences (*, $p<0.05$; **, $p<0.01$ and ***, $p<0.001$) within groups, i.e. 4°C vs. 21°C and 34°C vs. 21°C. Small circles show significant differences (o, $p<0.05$; oo, $p<0.01$ and ooo, $p<0.001$) vs. control, i.e. between effects of METH at the same temperature in NP-exposed and intact rats.

Table 2

Structural variability in BBB breakdown to [131]-Iodine induced by methamphetamine in intact rats and animals exposed to nanoparticles treatment

Brain regions	METH			METH+SiO2			METH+AgNP		
	4°C	21°C	34°C	4°C	21°C	34°C	4°C	21°C	34°C
1. Occipital cortex	0.23±0.04	0.86±0.04	1.12±0.08	0.89±0.09*	1.34±0.10*	1.78±0.12*	0.76±0.09*	0.98±0.06	1.48±0.06*
2. Parietal cortex	0.18±0.03	0.89±0.04	1.33±0.10	0.96±0.08*	1.28±0.08*	1.89±0.13*	0.88±0.08*	1.02±0.09	1.39±0.07
3. Cingulate cortex	0.17±0.04	0.98±0.10	1.45±0.12	0.98±0.05*	1.56±0.13*	1.88±0.09*	0.90±0.05*	1.17±0.10	1.65±0.12
4. Temporal cortex	0.20±0.07	0.76±0.07	1.21±0.08	0.88±0.05*	1.48±0.08*	1.95±0.05*	0.87±0.03*	1.23±0.08*	1.76±0.14*
5. Frontal cortex	0.24±0.04	0.90±0.12	1.34±0.06	0.87±0.10*	1.67±0.14*	2.04±0.16*	0.78±0.04*	1.34±0.06*	1.88±0.12*
6. Piriform cortex	0.13±0.02	0.78±0.05	1.33±0.03	0.96±0.09*	1.55±0.06*	2.21±0.14*	0.89±0.10*	1.32±0.08*	1.90±0.14*
7. Hippocampus	0.26±0.08	0.88±0.10	1.38±0.08	1.08±0.10*	1.76±0.14*	2.06±0.06*	0.98±0.09*	1.44±0.12*	1.76±0.14*
8. Thalamus	0.28±0.09	0.67±0.04	0.98±0.04	0.98±0.10*	1.66±0.05*	2.14±0.12*	0.89±0.10*	1.56±0.12*	1.90±0.13*
9. Hypothalamus	0.26±0.04	0.70±0.03	1.21±0.12	0.89±0.12*	1.56±0.15*	2.12±0.08*	0.82±0.12*	1.32±0.08*	1.88±0.08*
10. Cerebellum	0.11±0.04	0.89±0.08	1.54±0.05	1.21±0.08*	1.89±0.08*	2.23±0.08*	0.99±0.12*	1.45±0.13*	1.96±0.15*
11, Colliculi	0.22±0.04	0.87±0.10	1.32±0.08	0.90±0.12*	1.76±0.06*	2.14±0.12*	0.78±0.07*	1.22±0.06*	1.79±0.12*
12. Brain Stem	0.15±0.05	0.45±0.05	0.56±0.04	0.78±0.05*	0.98±0.08*	1.14±0.08*	0.68±0.07*	0.86±0.05*	0.97±0.08*

Values are mean±SEM obtained from 5 to 8 rats at each point. Asterisks show statistically significant differences between METH treatment at different ambient temperatures with and without additional exposure to nanoparticles (*, $p<0.05$). METH 4°C values are quite similar to that seen in saline control.

Mol Neurobiol. Author manuscript; available in PMC 2017 July 20.

Table 3

H-290/51-induced neuroprotection in METH neurotoxicity and its exacerbation by nanoparticle exposure

Groups	BBB breakdown		Brain Edema		Brain Pathology	
	Evans Blue, mg%	[131]-Iodine, %	Water content, %	% *f*	Neuronal Damage Abnormal cells	Astrocytic activation GFAP-positive cells
			Control			
H-290/51a	0.18±0.06	0.22±0.04	74.98±0.32	nil	2±1	2±2
H-290/51b	0.16±0.09	0.20±0.06	74.94±0.28	nil	1±2	3±2
			METH			
METH 21°C	1.89±0.21	2.34±0.23	76.34±0.21	+4	80±12	65±14
METH+H-290/51a	0.34±0.10**	0.45±0.02**	75.67±0.12*	+2	23±8**	28±8*
METH 34°C	2.67±0.26	3.45±0.23	77.45±0.12	+8	140±13	120±18
METH+H-290/51a	0.78±0.11**	0.98±0.08*	76.08±0.21**	+4	32±12**	36±18**
			Nanoparticles+METH			
SiO2 NPs						
METH 4°C	1.78±0.21	2.46±0.21	78.23±0.45	+12	220±34	190±32
METH+H-290/51b	0.56±0.08**	0.67±0.12**	75.34±0.12**	+1	29±8**	22±12**
METH 21°C	2.45±0.33	2.98±0.10	79.56±0.21	+17	367±43	345±28
METH+H-290/51b	0.60±0.08**	0.72±0.10**	75.67±0.22**	+2	34±18**	33±23**
METH 34°C	3.21±0.21	3.87±0.11	80.54±0.22	+23	456±28	398±12
METH+H-290/51b	0.68±0.10**	0.76±0.12**	75.87±0.19**	+2	40±21**	45±17**
Ag NPs						
METH 4°C	1.34±0.10	2.34±0.22	77.56±0.21	+8	160±33	187±27
METH+H-290/51b	0.46±0.10**	0.56±0.08**	75.45±0.13**	+1	18±10**	22±16**
METH 21°C	2.24±0.08	2.78±0.12	78.87±0.18	+13	308±26	298±32
METH+H-290/51b	0.56±0.08**	0.61±0.08**	75.38±0.11**	+1	22±8**	24±10**
METH 34°C	3.01±0.09	3.45±0.09	79.85±0.21	+16	412±34	325±28
METH+H-290/51b	0.62±0.08**	0.68±0.04**	75.46±0.10**	+1	28±10**	26±8**
Cu NPs						
METH 4°C	1.23±0.07	2.12±0.10	77.34±0.12	+8	140±23	167±24
METH+H-290/51b	0.38±0.08**	0.48±0.08**	75.48±0.18**	+1	18±7**	23±11**

Groups	BBB breakdown		Brain Edema		Brain Pathology	
	Evans Blue, mg%	[131]-Iodine, %	Water content, %	% *f*	Neuronal Damage Abnormal cells	Astrocytic activation GFAP-positive cells
METH 21°C	2.06±0.06	2.65±0.07	78.08±0.16	+12	280±18	245±26
METH+H-290/51b	0.46±0.08**	0.53±0.09**	75.56±0.12**	+1	24±8**	30±12**
METH 34°C	2.89±0.10	3.12±0.09	79.21±0.12	+21	378±23	312±20
METH+H-290/51b	0.54±0.10**	0.64±0.08**	75.63±0.11**	+2	32±12**	36±18**

Values are mean±SEM obtained from 5 to 8 rats at each point. Volume swelling (% *f*) is calculated according to Elliott & Jasper [31] and adjusted to nearest round figure for simplicity. a = single H-290/51 dose 50 mg/kg; b = three H-290/51 doses. Asterisks show values significantly different from their respective (*, $p<0.05$ and **, $p<0.00$).

Table 4

Physiological variables in different groups of rats exposed to METH at different temperatures with and without exposure to nanoparticles

Groups	Temperature, °C		Physiological variables				Heart Rate	Respiratory Rate
	Tc	Ts	MABP torr	Arterial pH	Arterial PaO2	Arterial PaCO2	beats/min	cycle/min
				Controls				
Saline 4°C	36.63±0.12	26.32±0.23*	108±7	7.38±0.03	80.76±0.21	34.57±0.11	320±9	65±6
Saline+H-290/51a	36.87±0.21	26.54±0.10	112±8	7.38±0.07	80.56±0.34	34.12±0.21	318±10	63±7
Saline 21°C	36.81±0.23	30.04±0.12	110±6	7.40±0.02	80.56±0.12	34.67±0.08	310±8	60±4
Saline+H-290/51a	36.78±0.21	31.12±0.21	116±5	7.38±0.05	80.34±0.21	34.56±0.18	308±14	64±9
Saline 34°C	37.01±0.12	33.21±0.21*	110±5	7.38±0.05	80.78±0.17	34.87±0.21	328±10	63±7
Saline+H-290/51a	37.23±0.21	33.34±0.12	108±8	7.37±0.09	80.56±0.18	34.89±0.17	320±12	60±8
				METH				
METH 4°C	32.34±0.08*	24.23±0.10*	92±6*	7.36±0.08	81.21±0.15	33.87±0.23	380±12*	68±6
METH+H-290/51a	31.43±0.32º	23.48±0.12	96±8	7.37±0.09	80.89±0.18	33.89±0.18	376±8	65±9
METH 21°C	39.78±0.14	28.34±0.13	120±7	7.39±0.08	81.76±0.23	32.34±0.18	420±13	75±10
METH+H-290/51a	39.61±0.12	28.02±0.10	118±6	7.37±0.05	81.09±0.13	33.23±0.18	388±12	67±9
METH 34°C	40.87±0.23*	33.45±0.21*	134±8	7.37±0.06	81.89±0.21	32.14±0.24	434±9	78±9
MTH+H-290/51a	40.49±0.34	33.21±0.28	132±10	7.36±0.09	81.56±0.32	32.54±0.28	430±8	75±6
				Nanoparticles+METH				
SiO2 NPs								
METH 4°C	33.34±0.21*	25.23±0.23*	98±6*	7.37±0.04	81.34±0.22	33.76±0.32	408±12	70±6
METH+H-290/51b	33.38±0.17	26.07±0.21	105±8	7.39±0.08	81.08±0.10	33.87±0.21	189±10	66±8
METH 21°C	40.12±0.20	30.34±0.31	134±6	7.39±0.06	81.88±0.34	32.19±0.33	430±8	78±4
METH+H-290/51b	39.77±0.18	30.12±0.21	123±10	7.38±0.09	81.23±0.28	33.29±0.14	418±12	74±10
METH 34°C	41.43±0.10*	34.45±0.12*	140±10	7.39±0.07	82.13±0.32	32.08±0.18	444±10	77±8
METH+H-290/51b	41.23±0.08	34.09±0.10	136±8	7.38±0.06	81.89±0.19	33.08±0.16	408±12	74±6
Ag NPs								
METH 4°C	31.46±0.32*	24.30±0.18*	90±4	7.36±0.07	81.44±0.32	33.23±0.29	389±12	67±8
METH+H-290/51b	30.56±0.32	25.21±0.08	94±6	7.37±0.08	81.08±0.32	33.87±0.21	367±10	65±9
METH 21°C	40.45±0.26	28.56±0.17	128±9	7.37±0.09	81.67±0.22	32.09±0.21	428±18	74±10
METH+H-290/51b	39.67±0.21	27.76±0.28	124±6	7.38±0.08	81.32±0.32	33.07±0.21	418±12	70±8

Groups	Temperature, °C		Physiological variables				Heart Rate	Respiratory Rate
	Tc	Ts	MABP torr	Arterial pH	Arterial PaO2	Arterial PaCO2	beats/min	cycle/min
METH 34°C	41.46±0.31	34.68±0.24*	134±8	7.35±0.09	82.05±0.34	32.18±0.33	430±8	76±8
METH+290/51b	40.98±0.08	34.03±0.09	128±9	7.37±0.09	81.89±0.32	32.89±0.23	424±10	70±6
Cu NPs								
METH 4°C	32.31±0.18*	25.33±0.21*	92±8	7.34±0.07	81.22±0.20	33.34±0.18	380±11	68±10
METH+H-290/51b	33.56±0.32	26.32±0.34	98±12	7.37±0.08	81.09±0.08	33.78±0.21	367±8	68±6
METH 21°C	40.67±0.17	28.86±0.31	120±6	7.37±0.05	81.57±0.34	32.31±0.18	401±11	72±6
METH+H-290/51b	39.88±0.21	27.28±0.43	122±4	7.38±0.06	81.32±0.18	33.02±0.21	389±10	70±12
METH 34°C	41.08±0.10	33.89±0.16*	138±8	7.36±0.09	81.98±0.21	32.34±0.10	416±7	75±10
MERH+H-290/51b	40.96±0.21	33.32±0.21	130±10	7.34±0.06	81.08±0.32	33.34±0.32	398±10	68±8

Values are mean±SEM obtained from 5 to 8 rats at each point. Tc = core body temperature; Ts = skin (tail) temperature; MABP = Mean arterial blood pressure; H-290/51a = single dose; H-290/51b = repeated doses. Asterisks show significant differences (*, $p<0.05$) within groups, i.e. 4°C vs. 21°C and 34°C vs. 21°C. Small circles show significant differences (o, $p<0.05$) between particle-exposed and particle-free, intact rats.